GEOPHYSICAL, GEOCHEMICAL AND MINERALOGICAL CHARACTERISTICS OF THE ALTERATION AND DEFORMATION HALO ABOVE A DIORITE-TONALITE INTRUSIVE COMPLEX AT NGATAMARIKI GEOTHERMAL FIELD

Steve Sewell[1], Mark P. Simpson[2], Michael F. Gazley[1,3] and Martha Savage[1]

[1] School of Geography, Environment and Earth Sciences, Victoria University, Wellington, NEW ZEALAND, 6140

[2] GNS Science, Wairakei Research Centre, 114 Karetoto Road - RD4, Taupo 3377

[3] RSC Mining and Mineral Exploration, 93 The Terrace, Wellington, 6011

Steven.Sewell83@gmail.com

Keywords: *Ngatamariki, geophysics, intrusive, hydrothermal minerals, rock chemistry*

ABSTRACT

To understand what controls the geophysical properties at the Ngatamariki geothermal field, New Zealand, particularly seismic velocity, an analysis of geophysical logs was undertaken. The geophysically-logged interval in the south of the field (well NM10) spans the propylitic altered, tuff-dominated, Tahorakuri Formation volcaniclastics and andesite. In contrast, the logged interval in the north of the field (NM9) spans the Tahorakuri Formation that experienced an earlier phase of potassic, advanced-argillic and phyllic alteration related to intrusion of a tonalite-diorite intrusive complex. Geochemical analyses of drill cuttings using portable X-ray fluorescence (pXRF) were obtained at a 5m depth interval spanning the logged intervals in each of the wells. These were combined with automated mineralogy using a Tescan Integrated Mineral Analyzer (TIMA) and quantitative X-ray diffraction (XRD) data on selected samples that provided quantitative mineralogy data. The geochemical and mineralogy data were then used to interpret the factors that affect the geophysical properties of the rocks. The Tahorakuri Formation was found to have markedly different geochemistry, mineralogy and petrophysical properties in the north of the field (NM9) compared to the south of the field (NM10) which we interpreted as due to the wide-spread quartz deposition and ductile deformation that took place during the intrusion of the tonalite-diorite complex. These processes reduced porosity within the Tahorakuri Formation in the north of the field, resulting in higher seismic velocity, higher density and higher resistivity relative to the south of the field (north (NM9) –average porosity of 7.5%, average P-wave velocity (Vp) 4.59 km/s, average density 2.64 g/cm^3, average resistivity 118 ohm.m versus south (NM10) – average porosity 18%, average Vp 3.78 km/s, average density 2.47 g/cm^3, average resistivity 20 ohm.m). The approximately 400m thick interval of Tahorakuri Formation in NM9 that overlies the intrusive has particularly low porosity (<5%) and consequent high seismic velocity (4.5–5.5 km/s), density (2.6–2.8 g/cm^3) and resistivity (500–1000 ohm.m). Abundant andalusite at the top of this interval provides evidence that the rock in this zone was >350 °C during the intrusive event. The inferred temperature, as well as deformation textures observed in an FMI log over this interval, suggest that the very low porosity is the result of ductile deformation. The interval between the andalusite altered tuff and the intrusive body appears to be relatively unaltered with abundant plagioclase and only subtle potassic alteration. Abundant small aperture (<0.1 mm), low-angle (<20° dip) fractures occur within this interval which are interpreted as being due to hydraulic fracturing due to pressure-transients that occurred within the lithostatic-pressured zone above the magma. The lack of alteration within this interval is interpreted as being due to the fluid within this zone being supercritical when the intrusive was emplaced with the low porosity/permeability that resulted from ductile deformation preventing further alteration as the magma cooled and during the present-day geothermal activity. The dataset provides insights into the changes in geophysical properties that occur close to intrusive bodies and has potential implications for geophysical imaging of magmatic intrusions and supercritical zones.

1. INTRODUCTION

1.1 Ngatamariki Geothermal Field

The Ngatamariki geothermal field is located on the eastern margin the central Taupo Volcanic Zone (TVZ) (Figure 1). Production on the Ngatamariki geothermal field began in 2013 with the commissioning of an 84 MW binary plant. Nearly 100% of the produced fluid at Ngatamariki is injected in two locations, ~1.5 km north and south of the production wells. Boseley et al. (2010) and Chambefort et al. (2016) described the conceptual hydrologic model for the Ngatamariki field. The highest measured temperatures (285 °C) and upflow area for the field are interpreted to occur between wells NM7, NM3 and NM2. Fluid outflows to the south, as demonstrated by the ~30 to 40°C cooler reservoir temperatures in the southernmost wells (NM6 and NM10). The deep reservoir is predominantly liquid-dominated (i.e. temperatures were below the boiling point in the natural state), but a small zone of boiling and two-phase (steam + liquid) fluid existed in the natural state around the NM2 and NM3 wells in the north of the field. Wells NM4 and NM8 in the north of the field encountered particularly low-permeability, manifest as low injectivity (< 1 t/h.bar) and conductive temperature profiles (linear with depth) in the natural state in NM4 and NM8. This has been interpreted as due to the presence of an intrusive body and its alteration halo in the north of the field (Chambefort et al., 2016). A low vertical permeability "clay-cap" overlies the deep reservoir and is characterised by smectite and smectite-illite alteration and conductive temperature profiles. Above the deep clay cap lies an intermediate aquifer system, hosted mainly in rhyolite lavas. Permeable connection between the intermediate aquifer and deep reservoir occurs between NM2, NM3 and NM1. Fluid therefore rises and boils from the reservoir into the intermediate aquifer in this area. Geothermal fluid mixes with cooler groundwaters within this zone and flows beneath a shallow clay cap discharging at thermal areas.

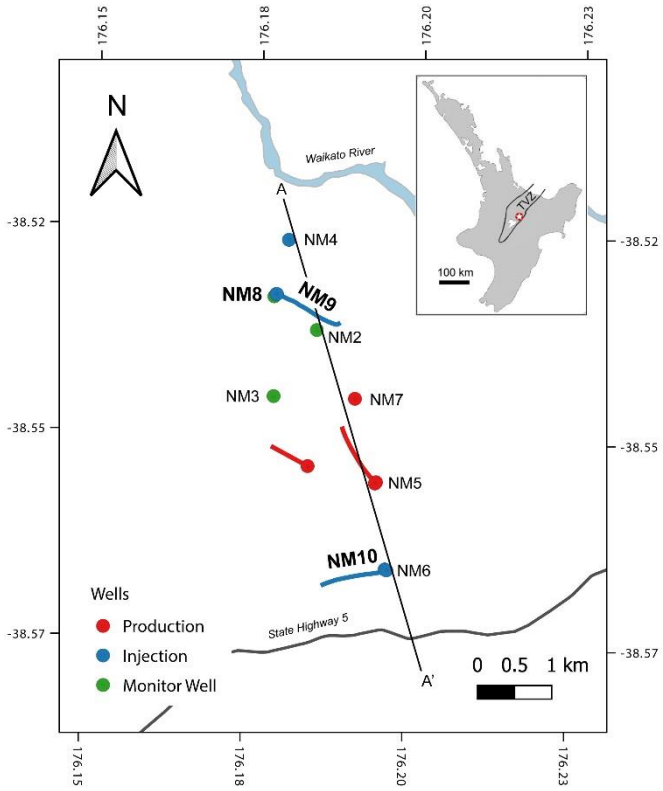

Figure 1. Map of the Ngatamariki field. Wells NM9 and NM10 (bold text) have geophysical logs discussed in this paper. A-A' shows the location of the cross-sections in Figure 2.

1.2 Geologic Setting

The upper 1 km of the Ngatamariki field consists mostly of surficial deposits (loosely compacted pumice and sediments), the Huka Falls Formation (lacustrine mudstones, siltstones, and sandstones), rhyolites, the Waiora Formation (volcaniclastic sediments) and the Whakamaru Group ignimbrite (formally known as the Wairakei Ignimbrite) (Figure 2). Below the Whakamaru Ignimbrite is the Tahorakuri Formation, which consists mostly of interlayered tuffs and volcaniclastic sediments with minor intervals of ignimbrites, rhyolites and basaltic to andesitic lavas, dykes and breccias. The Tahorakuri Formation lies between ~1–2 km below sea level (bsl) at Ngatamariki and is the main formation hosting the geothermal reservoir. Below the Tahorakuri Formation in the south of the Ngatamariki field is a sequence of andesitic lavas and breccias and the basement is Mesozoic-aged greywacke which has been intersected in one well (NM6) in the south of the Ngatamariki field at 3 km bsl (Chambefort et al., 2016). Alteration above 1 km bsl is variable, but often includes relatively high smectite and smectite-illite clay, particularly in the south of the Ngatamariki field (Boseley et al., 2010; Chambefort et al., 2016). Alteration below 1 km bsl within the reservoir is dominantly propylitic (mainly quartz, illite, chlorite, and epidote) except in the north of the field where an earlier phase of intrusion-related alteration occurs below the Whakamaru Group ignimbrite.

A unique feature of the Ngatamariki geothermal field is the intrusive complex (diorite-tonalite in composition) and its associated magmatic-hydrothermal alteration halo that has been intersected in three northernmost wells (NM4, NM8, and NM9) (Chambefort et al., 2017). This is the only young intrusive body that has been drilled within the TVZ to date. Age dating determined this intruded into the Tahorakuri Formation at ~0.65–0.71 Ma, before emplacement of the Whakamaru Group ignimbrites, and provided a heat source for the geothermal system operating during this time (Chambefort et al., 2016). Alteration of the Tahorakuri Formation above the intrusive complex reflects this magmatic phase ranging from potassic (biotite-magnetite ± K-feldspar) to advanced argillic (pyrophyllite ± minor andalusite ± topaz ± anhydrite ± rare alumino-phosphates and F-bearing minerals) and phyllic (quartz-muscovite-pyrite) assemblages (Chambefort et al., 2017). Phyllic alteration is the most wide-spread of the alteration types and is typified by intense silicification, white mica and pyrite (Chambefort et al., 2017).

1.3 Purpose of this study

The main purpose of this study was to understand what factors control seismic velocity in the field using geophysical logs from NM8, NM9 and NM10 (Figure 2) that would then serve as the basis for interpreting seismic velocity images obtained via seismic tomography. This paper however focuses on the differences in geophysical properties within the Tahorakuri Formation in NM9 and NM10 and provides detail on other geophysical properties (density and resistivity) for the Tahorakuri Formation which has implications for gravity and MT survey interpretation. The general approach to this study was to first identify geochemical units within the wells with similar geochemistry as determined from the closely spaced (5 m sampling) portable XRF analyses. Representative samples from these units were then selected for quantitative mineralogy analysis using an automated mineralogy scanning technique (TIMA) and quantitative XRD. These were then used in conjunction with the petrophysical logs to better understand the factors influencing the geophysical properties.

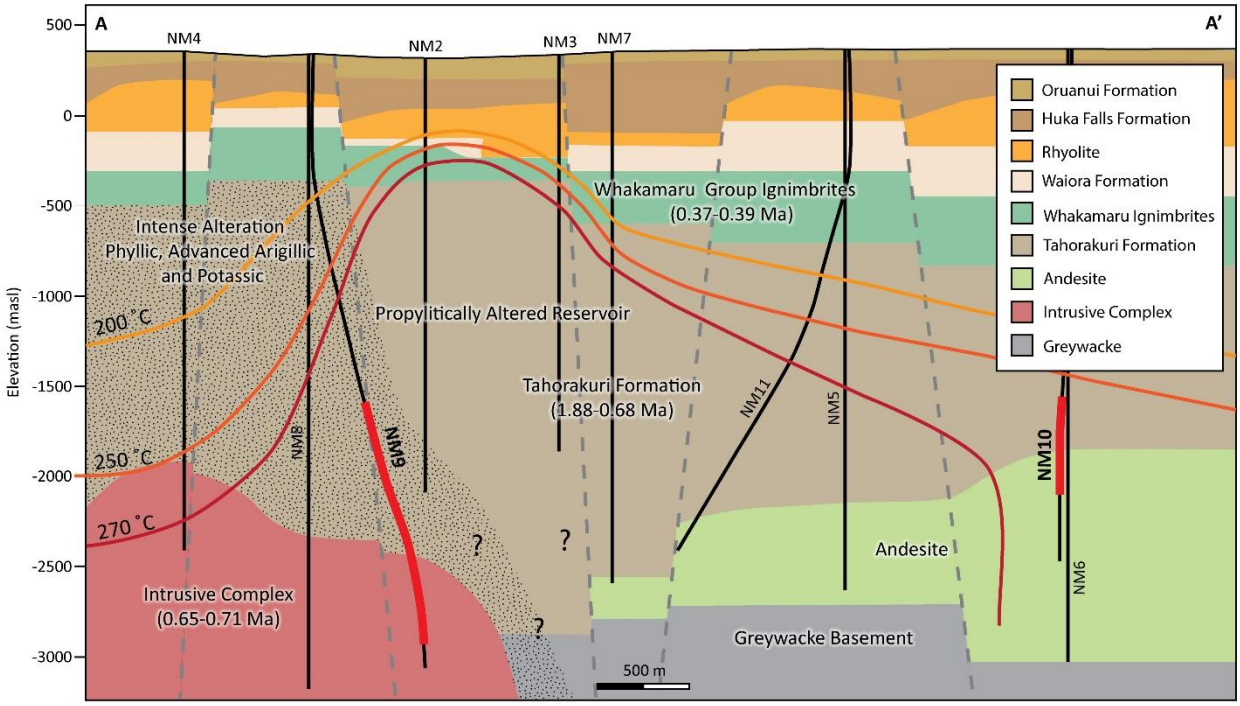

Figure 2. Geologic cross-section showing well tracks, the main geologic units and selected natural state temperature isotherms (Modified after Boseley et al. (2010) and Chambefort et al., 2016). The thick red lines on well tracks show the depth intervals of the petrophysical logs examined in this study.

2. DATA AND METHODS

2.1 Geophysical logging data

A suite of geophysical logs that generally included gamma, neutron porosity, resistivity, self-potential, density and formation imaging (FMI) were obtained in NM8, NM9 and NM10 (Wallis et al., 2009). All the geophysical logs provide measurements at depth intervals of ~0.15 m. All logs were acquired by Schlumberger as part of the post-drilling completion logging and testing. Most of the borehole sections logged had washout of less than eight inches (20 cms) and hence good seismic arrivals were recorded for most of the logged sections. Notable exceptions to this are several zones within NM10 where severe borehole washouts (>8 inches) resulted in complete loss of acoustic signal which are discussed further in the following sections. Manual review of the arrival picks in all wells provided an important quality check on the velocity data and minimised the number of incorrect picks due to cycle skipping and incorrect phase identification.

2.2 Portable XRF

The geochemistry of the altered host rocks was determined using an Olympus Delta pXRF instrument operating at 50 kV with a 4 W Ag X-ray tube. Data were acquired using both a 'geochem' and 'soil' mode. Most of the elemental data were obtained from the 'geochem' mode except for K. Data collection and processing methods are consistent with those outlined in Gazley and Fisher (2014), and references therein. Portable XRF analyses were made on washed drill cuttings at 5 m intervals and directly analysed in their plastic cuttings trays.

3.3 Automated mineralogy

The quantitative mineralogy of selected samples was determined from automated mineral mapping using a Tescan Integrated Mineral Analyser (TIMA) at the Australian Resources Research Centre, CSIRO, Perth, Australia. The instrument consists of a TESCAN MIRA3 field emission gun scanning electron microscope (FEG-SEM) operated at 25 kV and 6 nA, coupled with three Maxim PulseTor energy-dispersive spectroscopy (EDS) X-ray detectors. Energy dispersive spectrometry (EDS) measurements were made over an area of approximately 3 cm^2 on 25 mm diameter sample rounds with a step size of 10 µm, which generated approximately three million individual analyses. Mineral maps of the distribution of minerals were created by matching EDS analyses to the reference EDS via a spectra-matching library. Reference minerals are based on those previously identified from XRD, petrography and SEM. Where it was not possible to match an EDS spectrum to a reference spectrum, the pixel was marked as 'unclassified'. Most unclassified spectra are due to the analyses of more than one mineral grain resulting in a hybrid composition or portions of the sample with poor polish (pitted). By assigning EDS analyses into minerals, the abundance of each mineral could be quantified. The percentage of unclassified varied from 8–33% (average of 18%).

2.4 Quantitative XRD

Quantitative XRD on bulk-rock samples was performed on the same samples as the automated mineralogy. X-ray diffraction scans were made on powdered samples using a PANalytical XPertPro diffractometer (40 mA, 45 kV, Cu anode). Mineral phases present

ISSN 2703-4275

were identified using HighScore software. Mineral percentages were calculated using SIROQUANT software by comparing reference mineral profiles using the Rietveld method. All samples had 10% weight zinc oxide added prior to XRD analyses with this known amount used to refine mineral percentages. In most cases, the calculated amount of zinc oxide was within ±5%, which was considered adequate for the purposes of this study.

2.5 Cuttings depth correction

The drill-cutting sample depth is calculated rather than directly measured and is based on pumping rates, and losses or gains of fluid. This assumes cuttings travel at constant velocity with little-to-no mixing of cuttings during ascent. These assumptions mean that cuttings depth calculations can have large uncertainties (± 10s of m) compared to typical sampling intervals (<5 m). The cutting-depth calculations are particularly uncertain over intervals of partial losses (loss of fluid and cuttings from the well) where the amount of fluid and cuttings lost is often not accurately measured and where change in pressures within the well result in a change in fluid and cuttings velocity. This presents a challenge when trying to compare cuttings-based measurements to in-situ measurements.

To address this issue, the cuttings depths in this study were corrected using the K concentrations from pXRF by matching to gamma-ray logs (Figure 3). Gamma-ray logs measure the gamma ray emissions that are produced by naturally occurring radioactive isotopes U, Th and K in the rocks with sub-metre depth resolution. Since most samples in this study had either undetectable or very low U and Th concentrations (<20 ppm), the bulk of the gamma emissions is from K. Accordingly, the original calculated cutting depths can be adjusted to match between the gamma and K concentration in cuttings (Figure 3). To do this, marker horizons (prominent, and abrupt variations in the gamma response and K concentration) were identified and the depth of the cuttings were corrected to match that implied by the gamma ray log for these horizons. The cuttings depths between markers were corrected by assuming that samples between the marker horizons are equally spaced. The maximum shift in cuttings depth using this method was a shift of 40 m in NM9 at 2490 mRF. Partial loss of circulation (20–500 bbl/hr) occurred throughout the drilling of the logged section in NM9 which is the most likely reason for the large depth discrepancy. Correcting the cutting depths was an important step in being able to compare the pXRF, automated mineralogy, and XRD data to logging data obtained in the wells. This method of correcting cuttings depths may also have wider use in geological evaluation, for example obtaining more accurate stratigraphic offset data between wells which can be used to infer faults.

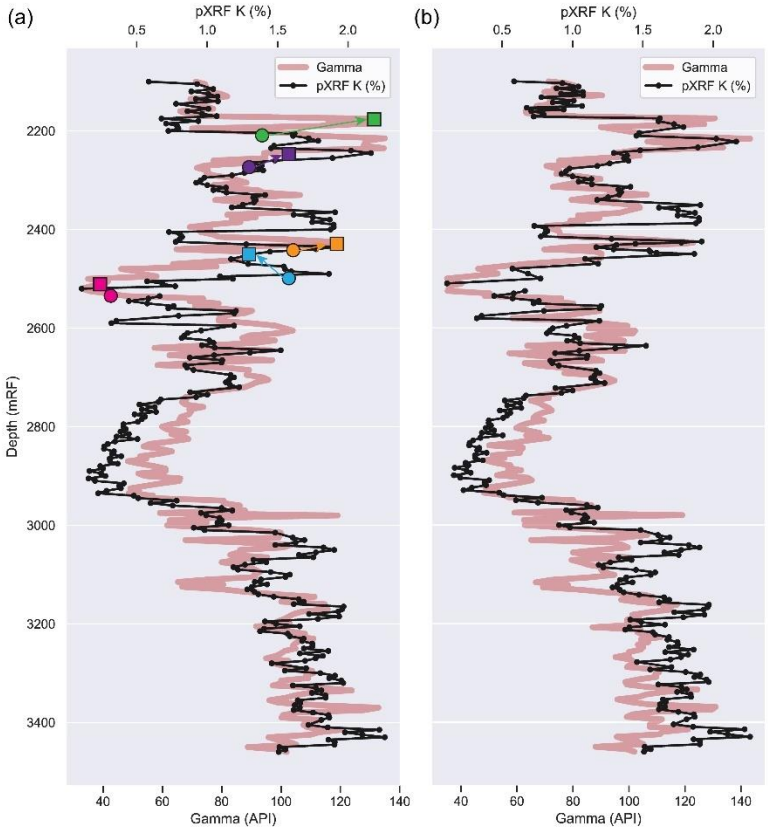

Figure 3. Example of the cutting-depth correction undertaken using the gamma ray log and pXRF K values for NM9. (a) Marker horizons (coloured circles and squares) where the pXRF K log and gamma log should align were visually identified. (b) The marker horizon cuttings depths were then assigned to be the same as the gamma log depths of the markers and the cuttings sample depths were recalculated so that samples between markers were equally spaced.

5. RESULTS

The full geochemical, mineralogical, and geophysical dataset is large and will be available in the first author's PhD thesis. Here we present summary logs for NM9 and NM10 that highlight the main mineral and elemental variations that result in differences in the geophysical properties of the Tahorakuri Formation across the geothermal field.

5.1 Seismic velocity, neutron porosity, geochemical and mineralogical properties

5.1.1 NM10

The Tahorakuri Formation in NM10 has an average P-wave velocity (Vp) of 3.78 km/s and average neutron porosity of 18% (Figure 4). The rocks are strongly propylitic altered with little mineralogical variation over the logged interval. Quartz is approximately 30-40%, albite ~25%, calcite 5–10%, illite ~8-12% and chlorite ~2-6%.

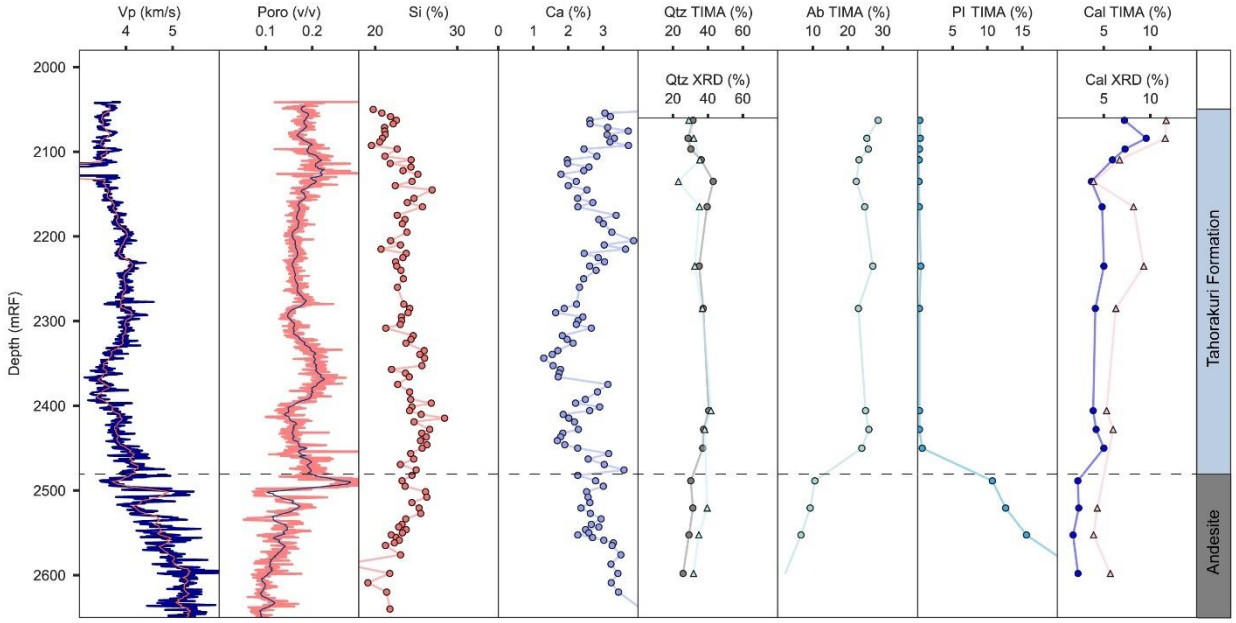

Figure 4. Selected geophysical logs - Vp and neutron porosity, pXRF data - silicon and calcium and automated mineralogy (circles) / XRD (triangles) mineral percentages: quartz (Qtz), albite (Ab), plagioclase (Pl) and calcite (Cal) for NM10.

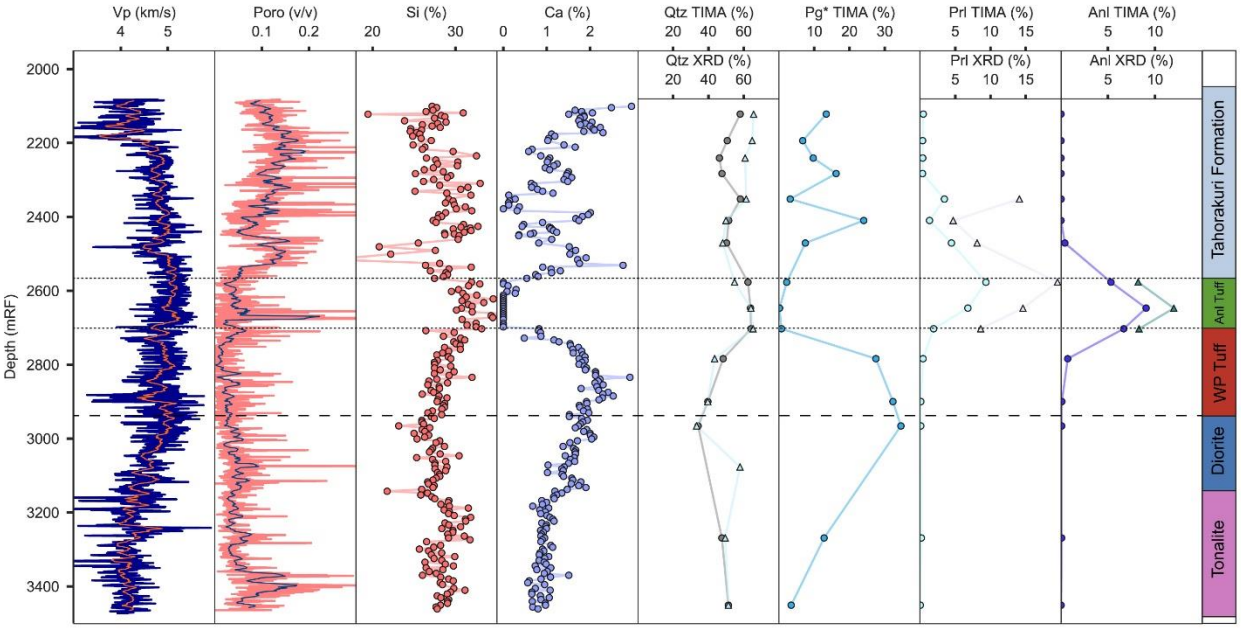

Figure 5. Selected geophysical logs - Vp and neutron porosity, pXRF data - Si and Ca, automated mineralogy (circles) and XRD data (triangles) – quartz, plagioclase (Pl), pyrophyllite (Prl) and andalusite (Anl) for NM9. The andalusite altered tuff ('Anl Tuff') and weak potassic altered tuff ('WP Tuff') are part of the Tahorakuri Formation that directly overlies the diorite-tonalite intrusive.

5.1.2 NM9

The Tahorakuri Formation in NM9 is substantially different from that in NM10 both in its geophysical properties, and its geochemical and mineralogical composition (Figure 5). The P-wave velocity (Vp) for the Tahorakuri Formation (including the 'Anl Tuff' and 'WP Tuff' units) averages 4.59 km/s and porosity averages 7.5%. In contrast to NM10, mineralogy in NM9 reflects both an older magmatic-hydrothermal system (potassic, advanced argillic, and phyllic) and the younger, neutral pH geothermal system. Silicon and

ISSN 2703-4275

quartz are higher and Ca lower than in NM10 suggesting deposition of quartz and removal of Ca has occurred during the low-pH, phyllic, advanced argillic and potassic alteration that occurred during the intrusive event.

Unlike in NM10, there are several distinct intervals in NM9 where the geophysical properties, and the geochemical and mineralogical composition abruptly change. The uppermost interval of the Tahorakuri Formation in NM9 (2100–2565 mRF) has the highest porosity (~7-15%) and lowest seismic velocity for the well (~4-5 km/s) (Figure 5). The interval from 2565–2940 mRF, which overlies the diorite-tonalite intrusive complex, has the lowest porosity (~0-5%) and highest seismic velocity (~4.5-5.5 km/s) for the Tahorakuri Formation. The upper section of this interval, from 2565–2700 m ('Anl Tuff') contains abundant pyrophyllite and andalusite indicating high-temperature (>375 °C), acidic conditions. Together, these two acidic-alteration minerals make up approximately ~5–35% of this interval. Calcium concentrations in this unit were undetectable (<0.1%) and corresponding low plagioclase (<1%) suggests that the acidic conditions leached most of the base cations from the rock. The seismic velocity and porosity for the unit between the andalusite-altered tuff and the intrusive ('WP Tuff') is similar to that for the 'And Tuff'; however, the geochemistry and mineralogy is markedly different. The 'WP Tuff' unit appears to be relatively unaltered when compared to the rest of the Tahorakuri formation in NM9 with high abundance of plagioclase and lower quartz. Acidic minerals are less abundant than the 'Anl Tuff' unit, but are still present in amounts that are quantifiable by automated mineralogy analyses (andalusite 0.6%, pyrophyllite 0.4%). The interval has evidence of weak potassic alteration with measurable occurrences of biotite (0.2% in the automated mineralogy data) and amphibole (2% automated mineralogy classified mostly as actinolite but with 0.2% hornblende, 2.5% XRD and identified as actinolite) for the Tahorakuri Formation occur within this unit.

5.2 Geophysical property differences in the Tahorakuri Formation for NM9 and NM10

Despite the primary lithologies (tuff-dominated) being the same, the geophysical properties of the Tahorakuri Formation are very different between wells NM10 and NM9 (Figure 6). The Tahorakuri Formation in NM9 has higher seismic velocity, density and resistivity which is mostly due to lower porosity. Overall, NM9 has an average porosity of 7.5%, average Vp 4.59 km/s, average density 2.64 g/cm^3, average resistivity 118 ohm.m whereas, NM10 has an average porosity 18%, average Vp 3.78 km/s, average density 2.47 g/cm^3, average resistivity 20 ohm.m). In NM9 an ~400 m interval spanning the andalusite altered tuff ('Anl Tuff') and the 'WP Tuff' unit (Figure 5) has particularly low porosity (<5%) and consequent high seismic velocity (4.5–5.5 km/s), density (2.6-2.8 g/cm^3) and resistivity (500–1000 ohm.m) (Figure 6). By contrast, the geophysical properties in NM10 are much less variable with porosity ranging from 13–22%, Vp from 3.2–4.2 km/s, density from 2.38–2.6 g/cm^3 and resistivity from 10–40 ohm.m. As the neutron porosity measures the total hydrogen content of the rock, it is possible that some of the porosity is associated with clay minerals which make up 6–14% of the rock. Sewell et al., 2021 describe how these differences in geophysical properties are imaged using seismic tomography, MT and gravity data.

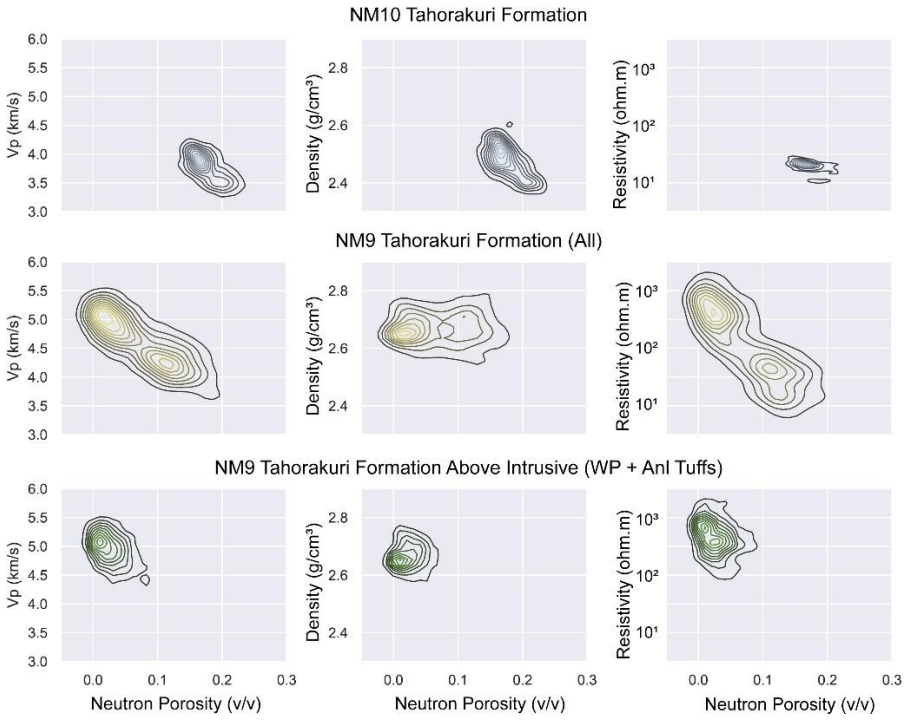

Figure 6. Kernel Density Element (KDE) plots of Vp, density and resistivity versus neutron porosity for the Tahorakuri Formation in NM10, NM9 and for the andalusite-altered ('Anl Tuff') and weakly-potassic altered ('WP Tuff') Tahorakuri formation only in NM9.

6. DISCUSSION

Pairing the geophysical data with quantitative geochemical and mineralogical data has revealed a number of factors and processes that have caused large differences in the geophysical properties of the Tahorakuri Formation between the north and the south of the Ngatamariki field. Figure 6 demonstrates that porosity is the main driver for the differences in geophysical properties in the logged

ISSN 2703-4275

sections of these wells. The lower porosity, and corresponding increases in geophysical properties in NM9, appears to be due to both alteration and ductile deformation associated with the intrusive complex.

It appears that quartz deposition during the intrusive event has been a significant factor in lowering porosity in the Tahorakuri Formation in NM9. The average quartz content for the Tahorakuri Formation in NM10 is ~30 to 40 % whereas in NM9 it is ~45 to 65% (Figure 4 and Figure 5). Given the pervasive nature of phyllic alteration in the north (Chambefort et al., 2017), this quartz deposition likely extends over a wide region in the north below the Whakamaru Group Ignimbrites (Figure 2). However, quartz deposition alone cannot explain the lowest porosity section of the Tahorakuri Formation in NM9 (the 'And Tuff' and 'Met Tuff' that overlie the intrusive) as quartz content is similar to the uppermost section of Tahorakuri Formation for the andalusite-altered tuff ('Anl Tuff') and decreases within the 'WP Tuff' unit that directly overlies the intrusive (Figure 5). Instead, the very low porosities and corresponding very high Vp, density and resistivity for these units are best explained by ductile deformation during the intrusive event. The presence of andalusite in the 'Anl Tuff' unit and weak potassic alteration in the 'WP tuff' provides evidence for temperatures likely above the brittle-ductile transition (>375°C, Chambefort et al., 2017; Violay et al., 2017) and this is inferred to have caused ductile/plastic deformation of these units which led to the closing of most of the pore space and reduced permeability; as proposed by Christenson et al., (1997) for Ngatamariki.

Further evidence of ductile/plastic deformation comes from an FMI image log obtained in NM9 (Figure 7). Deformed textures, characterised by heterogenous resistivity and a lack of volcanoclastic clasts, were identified throughout the 'Anl Tuff' unit (Halwa, 2013). Texture within the 'WP Tuff' unit that lies between the andalusite-altered tuff ('Anl Tuff') and the intrusive is characterised by abundant, small-aperture fractures (average aperture of 0.07 mm compared with an average of 0.97 mm for all fractures within the well) (Figure 7a). Approximately one quarter of the fractures within the unit are low-angle (<20° dip, mean dip 10°, with no well-defined strike direction from 2730–2930 mRF), suggesting a different stress regime than that which produced the bulk of fractures (dip >50°, dominant NE-SW striking) (Figure 7b and Figure 7c). The most likely explanation for this is hydraulic fracturing that occurred during the intrusive event when pressures close to the intrusive were lithostatic and pressure transients (e.g. during the release of gas from the magma) caused fracturing as was proposed by Christenson et al., (1997) and as observed and modelled in porphyry systems (e.g. Fournier, 1999). Similar abundant low-angle fractures were identified in an FMI log from the Kakkonda geothermal system in Japan where present-day measured temperatures are 350–400°C above a granitic intrusion where measured temperatures are >500°C which were attributed to hydraulic fracturing caused by the dehydration front associated with contact metamorphism (Muraoka et al., 1998). It is possible that quartz deposition in this zone may have played a role in lowering porosity however since the plastic deformation would have occurred first, and quartz is observed to be lower in the 'WP Tuff' unit, this would presumably have been secondary to the closing of pore space by ductile deformation.

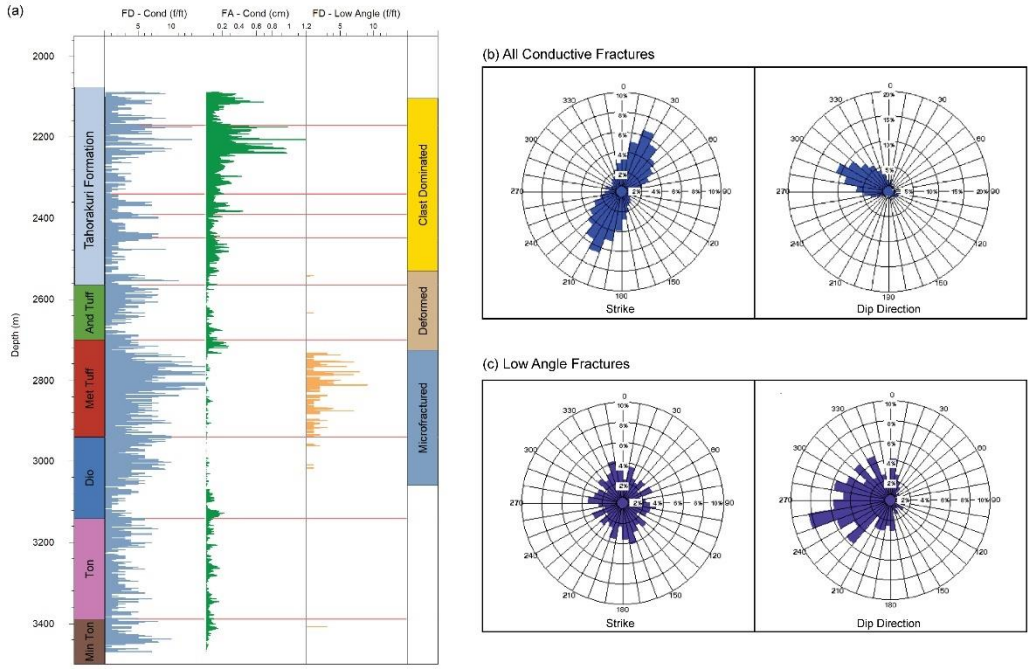

Figure 7. (a) Fracture data (FD Cond = Conductive Fracture Density, FA Cond = Conductive Fracture Aperture, FD – Low Angle = Low Angle Fracture Density. Fracture density units are fractures per foot, and textural zones (rightmost column) identified from an analysis of the FMI log in NM9. (b) Fracture strike and dip direction for all conductive fractures in the well and (c) the low angle fractures that are mostly within the 'Met Tuff' unit. Modified from Halwa (2013).

The apparent lack of alteration within the 'WP Tuff' unit can be explained by the fluids within this zone being at a supercritical condition. The zonation of low-pH fluid above a neutral-pH supercritical fluid zone has been observed at the Krafla field where wells have produced both very acidic fluids in the zone overlying the supercritical zone and supercritical fluids themselves (Heřmanská et al., 2019). Heřmanská et al., 2019 modelled that no alteration would take place within the supercritical zone and that condensation above the supercritical zone would form a very low-pH fluid through formation of HCl and SO_4 acid. The andalusite-pyrophyllite

ISSN 2703-4275

zone overlying a relatively unaltered zone ('WP Tuff') at Ngatamariki in NM9 appears to reflect this process. Ductile deformation when the fluid was in a supercritical state within the 'WP Tuff' unit would have resulted in closure of porosity and lowering of permeability which in turn would have limited further fluid-rock reactions once the intrusive had cooled and during the formation of the present-day geothermal system.

Alteration within the logged section of the Tahorakuri Formation in NM10 is representative of the lower temperature (250–270 °C), deep margins of the reservoir. Currently no logging data exists for the central, higher temperature (270–280 ˚C) part of the reservoir (NM7-NM11 area), and therefore there is some uncertainty whether there is significant variation in geophysical properties within the Tahorakuri Formation towards the hotter upflow area. However, widespread deposition of quartz that reduces the matrix porosity, as is seen in the north of the field, is not expected above 2 km and <350 ˚C based on quartz solubility controls. There is also some uncertainty as to the extent of deformation and alteration of the Tahorakuri Formation south of the intrusive complex

7. CONCLUSION

The intrusive event in the north of the Ngatamariki field has significantly altered the geochemical, mineralogical and physical properties of the tuff-dominated Tahorakuri Formation. Porosity in the north of the field appears to have been lowered by both wide-spread quartz deposition and ductile deformation in a zone extending several hundred metres above the intrusive complex. The lower porosity has increased the seismic velocity, density and resistivity in the north of the field within the Tahorakuri Formation. The lowest porosities (0–5%), highest seismic velocities (Vp 4.5–5.5 km/s), highest densities (2.6–2.8 g/cm^3) and highest resistivities (100–1000 ohm.m) within the Tahorakuri Formation occur above the tonalite/diorite intrusion in NM9. Evidence from mineralogy and an FMI log suggest this particularly low porosity is due mostly to ductile deformation when past-temperatures within this zone exceeded 350 °C and the fluid was likely in a supercritical state. The study shows that major geophysical property changes take place hundreds of metres above and adjacent to the magmatic intrusions that provide the heat source of many geothermal systems.

ACKNOWLEDGEMENTS

The authors wish to acknowledge the Rotokawa Joint Venture (Mercury Energy and Tahaura North No. 2) for providing the logging data and access to drill cuttings. GNS Science are thanked for facilitating the pXRF measurements, particularly Patricia Durance.

REFERENCES

Boseley, C., Cumming, W., Urzúa-Monsalve, L., Powell, T., & Grant, M. (2010). A resource conceptual model for the Ngatamariki geothermal field based on recent exploration well drilling and 3D MT resistivity imaging. *Proceedings World Geothermal Congress.*

Chambefort, I., Buscarlet, E., Wallis, I., & Sewell, S. (2016). Ngatamariki geothermal field, New Zealand: Geology, geophysics, chemistry and conceptual model. *Geothermics.*

Chambefort, I., Lewis, B., Simpson, M. P., Bignall, G., Rae, A. J., & Ganefianto, N. (2017). Ngatamariki Geothermal System: Magmatic to Epithermal Transition in the Taupo Volcanic Zone, New Zealand. *Economic Geology*, *112*(2), 319–346.

Christenson, B. W., Mroczek, E. K., Wood, C. P., & Arehart, G. B. (1997). Magma-ambient production environments: PTX constraints for paleo-fluids associated with the Ngatamariki diorite intrusion. *Proceedings of the 19th New Zealand Geothermal Workshop*, 87–92.

Fournier, R. O. (1999). Hydrothermal processes related to movement of fluid from plastic into brittle rock in the magmatic-epithermal environment. *Economic Geology*, *94*(8), 1193–1211.

Gazley, M. F., & Fisher, L. A. (2014). A review of the reliability and validity of portable X-ray fluorescence spectrometry (pXRF) data. *Mineral Resource and Ore Reserve Estimation–The AusIMM Guide to Good Practice*, *69*, 82.

Halwa, L. (2013). *FMI Image Interpretation Report. Mighty River Power. Ngatamariki-9.*

Heřmanská, M., Stefánsson, A., & Scott, S. (2019). Supercritical fluids around magmatic intrusions: IDDP-1 at Krafla, Iceland. *Geothermics*, *78*, 101–110.

Muraoka, H., Uchida, T., Sasada, M., Yagi, M., Akaku, K., Sasaki, M., Yasukawa, K., Miyazaki, S. I., Doi, N., Saito, S., Sato, K., & Tanaka, S. (1998). Deep geothermal resources survey program: Igneous, metamorphic and hydrothermal processes in a well encountering 500°C at 3729 m depth, Kakkonda, Japan. *Geothermics*, *27*(5–6), 507–534.

Sewell, S., Savage, M., Townend, J., Hopp, C., Mrocek, S., Graham, K. (2021). Imaging the alteration and deformation halo above the diorite-tonalite intrusive at the Ngatamariki Geothermal Field. *Proceedngs of the New Zealand Geothermal Workshop.*

Violay, M., Heap, M. J., Acosta, M., & Madonna, C. (2017). Porosity evolution at the brittle-ductile transition in the continental crust: Implications for deep hydro-geothermal circulation. *Scientific Reports*, *7*(1), 7705.

Wallis, I., McCormick, S., Sewell, S., & Boseley, C. (2009). Formation assessment in geothermal using wireline tools-application and early results from the Ngatamariki Geothermal Field, New Zealand. *Proceedings of the New Zealand Geothermal Workshop* ….